Int. J. Heat Mass Transfer. Vol. 8, pp. 43–53. Pergamon Press 1965. Printed in Great Britain

COMBINED FORCED AND NATURAL CONVECTION FLOW FOR THE WEDGE GEOMETRY

R. C. GUNNESS JR.* and B. GEBHART†
Cornell University, Ithaca, New York

(*Received* 20 *April* 1964 *and in revised form* 1 *July* 1964)

Abstract—This paper considers simultaneously the phenomena of forced and natural flow effects over an isothermal wedge. The analysis is restricted to situations in which the natural convection effects may be considered as a perturbation of the purely forced flow situation. Using this technique, a number of wedge angles are considered for laminar boundary-layer type flow. A Prandtl number of 0·73 was used and numerical results are presented for calculating surface shear and heat-transfer rates. Boundary-layer separation is also considered.

NOMENCLATURE

B, coefficient of volume expansivity $\left[= -\left(\frac{1}{\rho}\frac{\partial p}{\partial t}\right)_p\right]$;
g_x, component of gravity in the x-direction;
g_y, component of gravity in the y-direction;
p, static pressure;
t, temperature;
u, velocity component in the x-direction;
v, velocity component in the y-direction;
x, co-ordinate along the wedge surface, starting from the leading edge;
y, co-ordinate normal to plate surface;
α, thermal diffusivity;
β, measure of included wedge angle (i.e. $\pi\beta$ equals wedge angle in radians);
ϵ_1, ϵ_2, expansion parameters [see equations (19) and (20)];
μ, viscosity;
ν, kinematic viscosity;
ρ, density.

Subscripts

e, refers to flow region external to boundary layer;
w, refers to wall condition.

INTRODUCTION

THE SUBJECT of combined forced and natural convection has recently been investigated in some detail. This flow regime is concerned with circumstances wherein both the natural and forced mechanisms of the flow must be considered simultaneously. The natural flow originates from body force variations in the fluid, whereas the forced convection is generally induced by moving a body through a quiescent fluid or by forcing a fluid past a stationary body.

For the mixed convection flow over a flat surface a number of important investigations have been made. Tanaev [1] published an approximate analytical analysis for laminar, compressible, mixed flow of air over an inclined flat plate. The external flow was assumed parallel to the plate for all plate inclination angles. His analysis is for low Mach numbers and for situations where the buoyancy effects could be considered small relative to the forced flow effects.

Acrivos [2] employed the Pohlhausen–von Kármán momentum integral method to consider incompressible laminar flow over a vertical, isothermal plate with buoyancy effects included. The form of the velocity and temperature profiles for the combined convection were assumed to be the sum of the purely forced and natural convection profiles. This assumption is suspect however due to the basic non-linearity of viscous flow problems. Numerical results were reported for the heating and cooling of upward flow past the vertical plate for Prandtl numbers of 0·73, 10 and 100. The influence of natural convection on separation showed that heating of

* Research Assistant.
† Professor of Mechanical Engineering.

the upward flow stabilizes the boundary layer, whereas cooling hastens the appearance of separation.

Sparrow and Gregg [3] attacked the isothermal vertical plate problem, considered by Acrivos, by a different approach. They perturbed the equations of the purely forced flow circumstance to include small effects of buoyancy. This study considered both the cases where the buoyancy effects are parallel and opposed to the external flow. The analysis was restricted to laminar boundary-layer flow and calculations were made for Prandtl numbers of 10, 1 and 0·01. For fluids with larger Prandtl numbers the effects of buoyancy were found to be of smaller importance.

Szewczyk [4] also investigated combined flow over a vertical isothermal surface, considering two types of perturbations. First, purely forced flow was perturbed to include small buoyancy effects. This portion of the analysis is similar to that of [3]. However, Szewczyk considered as well the second-order term of the perturbation series. The second part of the analysis considers a perturbation of the natural convection flow to include small forced flow effects and the second, as well as the first-order perturbation term is included. Results were tabulated for Prandtl numbers of 0·01, 0·72, 1·0, 5·0 and 10·0.

The case of laminar, mixed flow over an isothermal, horizontal flat plate has been investigated by Mori [5] and by Sparrow and Minkowycz [6]. Mori considered the case for a Prandtl number of 0·72 while Sparrow and Minkowycz considered Prandtl numbers of 0·01, 0·7 and 10. In both [5] and [6] the technique of perturbing the purely forced flow equations to include small effects of buoyancy was applied. Both investigations present formulae for calculating the shear stress and heat-transfer rate in the mixed flow regime.

Gill and Del Casel [7] considered the influence of buoyancy for flow over a horizontal flat plate with a non-uniform temperature at the surface. They found that the boundary-layer equations had a similarity solution for a surface temperature varying as one over the square root of distance from the leading edge. With this surface condition, however, there is no local heat transfer. The physical significance of this situation is not apparent. Prandtl numbers of 0·01, 0·72 and 10 were considered. For the plate temperature greater than that of the fluid external to the boundary layer, the parallel velocity component was found to increase and temperature to decrease for flow over the top of the plate, relative to the corresponding forced flow results. The opposite effects were encountered for the bottom of the plate. These results are in agreement with those found in [5] and [6]. It was similarly observed that buoyancy has less influence as the Prandtl number is increased.

The first investigation concerning mixed flow over a wedge was that of Sparrow, Eichhorn and Gregg [8]. They obtained a solution for the mixed convection boundary-layer flow for several special cases under which a similarity transformation was possible. They found that isothermal and uniform-flux surface conditions resulted in similarity transformations for vertical wedges having included wedge angles of 120° and 135°, respectively. In their analysis they neglected buoyancy effects in the direction normal to the wedge surface (this assumption is later discussed in the analysis). The Prandtl number was taken to be 0·73 for all cases considered.

Brindley [9] considered an approximate technique to solve the ordinary differential equations encountered by Sparrow, Eichhorn and Gregg. His primary intent, however, was the comparison of his approximate method with respect to known numerical solutions.

The present communication considers mixed flow over isothermal wedges for a variety of included angles. The regime considered is incompressible, laminar, boundary-layer flow with a Prandtl number of 0·73. Two types of wedge orientation will be treated. The first case will be for horizontal wedges, i.e. the plane of symmetry normal to the body force, shown in Fig. 1 as Case A. The second case is for vertical wedges, shown in Fig. 1 as Case B.

For the case of the purely forced convection flow over a wedge, Falkner and Skan [10] reduced the general boundary-layer continuity and motion equations into a single ordinary differential equation by the proper choice of a similarity variable. Later, Eckert [11] transformed the boundary-layer energy equation, for

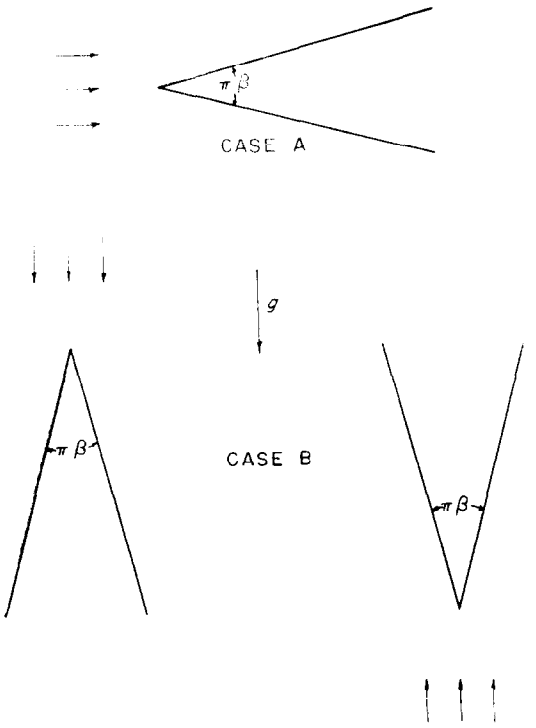

FIG. 1. Wedge configurations.

the purely forced flow, into an ordinary differential equation by using the same similarity variable found in the Falkner–Skan treatment.

As previously indicated, a similarity transformation for the mixed flow over a wedge is only possible for two special wedge cases. Therefore, the method used by the present writers is to perturb the Falkner–Skan and Eckert equations to include small effects of buoyancy. By this technique a number of the important mixed flow phenomena not amenable to similarity solutions are considered.

ANALYSIS

With reference to Fig. 1, the boundary-layer equations are:

continuity:

$$\frac{\partial u}{\partial x} + \frac{\partial v}{\partial y} = 0 \tag{1}$$

motion in the x and y direction:

$$\rho\left[u\frac{\partial u}{\partial x} + v\frac{\partial u}{\partial y}\right] = -\frac{\partial p}{\partial x} + \mu\frac{\partial^2 u}{\partial y^2} + X \tag{2}$$

$$\frac{\partial p}{\partial y} = Y \tag{3}$$

energy:

$$u\frac{\partial t}{\partial x} + v\frac{\partial t}{\partial y} = \alpha\frac{\partial^2 t}{\partial y^2} \tag{4}$$

with boundary conditions:

$$\begin{aligned} &y = 0; \quad u = v = 0, \quad t = t_w \\ &y \to \infty; \quad u \to u_e(x), \quad t \to t_e \end{aligned} \tag{5}$$

where

$X = \rho g_x$—body force in the x-direction (6)

$Y = \rho g_y$—body force in the y-direction (7)

These equations are valid for incompressible flows with Reynolds numbers of such magnitude that the boundary-layer approximations are valid. However, to account for buoyancy effects, we may consider density variations in the body force terms, yet maintaining the incompressible equation for fluids for which the volume expansivity is small. Thus, the density, except in the body force terms, will be taken equal to the external flow value (i.e. ρ_e).

Equations (6) and (7) may be rewritten such that:

$$X = \rho g_x = g_x\,[(\rho - \rho_e) + \rho_e] \tag{8}$$

$$Y = \rho g_y = g_y\,[(\rho - \rho_e) + \rho_e] \tag{9}$$

where

$$(\rho - \rho_e) = -\rho_e\,\beta(t_w - t_e)\,\theta \quad \text{for} \quad t - t_e \text{ small}$$

and

$$\theta = \frac{t - t_e}{t_w - t_e}$$

Substituting equations (8) and (9) into equations (2) and (3) and equating the cross derivatives of p from the two equations ($\partial p/\partial y \neq$ constant)

$$u\frac{\partial^2 u}{\partial x\,\partial y} + v\frac{\partial^2 u}{\partial y^2} = \nu\frac{\partial^3 u}{\partial y^3} - g_x B(t_w - t_e)\frac{\partial \theta}{\partial y} + g_y B(t_w - t_e)\frac{\partial \theta}{\partial x} \tag{10}$$

We define a stream function, $\psi(x, y)$, which identically satisfies the continuity equation

$$\frac{\partial \psi}{\partial y} = u, \quad \frac{\partial \psi}{\partial x} = -v \qquad (11), (12)$$

Equations (10) and (4) may be written in terms of the stream function as:

$$\left(\frac{\partial \psi}{\partial y}\right)\left(\frac{\partial^3 \psi}{\partial x\, \partial y^2}\right) - \left(\frac{\partial \psi}{\partial x}\right)\left(\frac{\partial^3 \psi}{\partial y^3}\right) = \nu \frac{\partial^4 \psi}{\partial y^4} - g_x B(t_w - t_e)\frac{\partial \theta}{\partial y} + g_y B(t_w - t_e)\frac{\partial \theta}{\partial x} \qquad (13)$$

$$\frac{\partial \psi}{\partial y}\frac{\partial \theta}{\partial x} - \frac{\partial \psi}{\partial x}\frac{\partial \theta}{\partial y} = a \frac{\partial^2 \theta}{\partial y^2} \qquad (14)$$

The boundary conditions corresponding to (5) are:

$$\left.\begin{aligned} &y = 0;\ \frac{\partial \psi}{\partial y} = 0,\ \frac{\partial \psi}{\partial x} = 0,\ \theta = 1 \\ &y \to \infty;\ \frac{\partial \psi}{\partial y} \to u_e(x),\ \theta \to 0 \end{aligned}\right\} \qquad (15)$$

In the case of purely forced flow u/u_e is simply a function of η where $\eta = (y/2)\sqrt{(u_e/\nu x)}$ and $u_e(x) = Cx^m$ is the velocity external to the boundary layer as determined from potential theory. For our case u/u_e is no longer a function of η and it was found necessary to introduce the following transformation of variables $(x, y) \to (\epsilon_1, \epsilon_2, \eta)$, so that a perturbation method could be applied which considers both the $\partial\theta/\partial y$ and $\partial\theta/\partial x$ terms simultaneously in equation (13). Expanding u/u_e then in a double power series about $\epsilon_1 = \epsilon_2 = 0$ and integrating equation (11) for ψ we find

$$\frac{\psi}{\sqrt{(u_e \nu x)}} = [f_0(\eta)] + [\epsilon_1(x) F_1(\eta) + \epsilon_2(x) G_1(\eta)] + \ldots \qquad (16)$$

Similarly for θ we have

$$\theta = \theta_0(\eta) + [\epsilon_1(x) H_1(\eta) + \epsilon_2 I_1(\eta)] + \ldots \qquad (17)$$

Where $\epsilon_1(x)$, $\epsilon_2(x)$ are expansion variables (assumed functions of x only) and $f_0(\eta)$, $F_1(\eta)$, $G_1(\eta)$, $\theta_0(\eta)$, $H_1(\eta)$, $I_1(\eta)$, etc. are the expansion coefficients. Since we are considering only a first-order perturbation analysis, only the first three terms in equations (16) and (17) will be considered. The boundary conditions (15) are

$$\left.\begin{aligned} &\eta = 0:\ f_0 = f_0' = 0,\ \theta_0 = 1 \\ &F_1 = F_1' = 0,\ H_1 = 0 \\ &G_1 = G_1' = 0,\ I_1 = 0 \\ &\eta \to \infty;\ f_0' \to 2,\ f_0'' \to 0,\ \theta_0 \to 0 \\ &F_1' \to 0,\ F_1'' \to 0,\ F_1 \to 0 \\ &H_1 \to 0,\ I_1 \to 0 \end{aligned}\right\} \qquad (18)$$

Substitutions of equations (16) and (17) into equations (13) and (14) yields the form of the expansion variables $\epsilon_1(x)$ and $\epsilon_2(x)$. They are chosen so that the expansion coefficients $F_1(\eta)$, $G_1(\eta)$, $H_1(\eta)$, and $I_1(\eta)$ are indeed functions of η only. Hence:

$$\epsilon_1(x) = \frac{Gr(x)}{Re^2(x)} \qquad (19)$$

$$\epsilon_2(x) = \frac{Gr(x)}{Re^{5/2}(x)} \qquad (20)$$

where

$$Gr(x) = \pm \frac{|g|\, B(t_w - t_e)x^3}{\nu^2}$$

$$Re(x) = \frac{u_e x}{\nu}$$

The $\pm$ sign above is discussed in the Appendix.

With ϵ_1 and ϵ_2 as given in equations (19) and (20), one obtains ordinary differential equations by comparing like powers of the expansion variables in both the motion and the energy equations. Setting

$$g_x = \pm \gamma |g| \quad \text{and} \quad g_y = \pm \lambda |g|$$

(see Appendix for values of λ and γ) we obtain from the motion equation three ordinary differential equations. These may be integrated once between η and ∞ to yield:

$$f_0''' + (m+1) f_0 f_0'' + 8m\left(1 - \frac{f_0'^2}{4}\right) = 0 \qquad (21)$$

$$F_1''' = 8\gamma\theta_0 + 2f_0' F_1' - (m+1) f_0 F_1'' + 3(m-1) f_0'' F_1 \qquad (22)$$

$$G_1''' = (1-m)(8\lambda)\left(\eta\,\theta_0 + \int_0^\eta \theta_0\,d\eta\right) + (4m-2)f_0''\,G_1 + (1-m)\,G_1' f_0' - (m+1)\,f_0\,G_1'' \quad (23)$$

Similarly, using equations (19) and (20) and substituting equation (17) into equation (14) and comparing like powers of the ϵ's, one obtains from the energy equation the equations for the coefficients:

$$\theta_0'' + (m+1)(Pr) f_0\,\theta_0' = 0 \quad (24)$$

$$H_1'' = (Pr)(2-4m)\,H_1 f_0' - (Pr)(m+1)\,H_1' f_0 - (Pr)(3-3m)\,\theta_0'\,F_1 \quad (25)$$

$$I_1'' = (Pr)(1-5m)\,I_1 f_0' + 2(Pr)(2m-1)\,\theta_0' G_1 - (Pr)(m+1)\,I_1' f_0 \quad (26)$$

The solution to equations (21), (22), (23), (24), (25) and (26) with boundary conditions (18) yield the coefficients in equations (16) and (17).

It is seen that equation (21), together with boundary conditions (18), is the Falkner–Skan [10] equation. Similarly, equation (24) is the Eckert [11] energy equation.

In summary, the velocity field for the combined forced and natural convection flow is found from differentiation of equation (16) to yield:

$$\frac{u}{u_e}(\epsilon_1, \epsilon_2, \eta) = \frac{\partial\psi}{\partial y} = \frac{1}{2}\left[f_0'(\eta) + \epsilon_1(x)\,F_1'(\eta) \pm \frac{\epsilon_1(x)}{\sqrt{[Re(x)]}}\,G_1'(\eta)\right] \quad (27)$$

The temperature field for the combined phenomena from (17) is:

$$\theta(\epsilon_1, \epsilon_2, \eta) = \theta_0(\eta) + \epsilon_1(x)\,H_1(\eta) \pm \frac{\epsilon_1(x)}{\sqrt{[Re(x)]}}\,I_1(\eta) \quad (28)$$

The local wall shear stress and heat-transfer rate for the mixed flow becomes, making use of equation (20):

$$\tau(x) = \mu\left(\frac{\partial u}{\partial y}\right)_{y=0} = \mu\frac{u_e}{4}\sqrt{\left(\frac{u_e}{\nu x}\right)}\left\{ f_0'' + \epsilon_1(x)\,F_1'' \pm \frac{\epsilon_1(x)\,G_1''}{\sqrt{[Re(x)]}}\right\}_{\eta=0} \quad (29)$$

$$\dot{q}''(x) = -k\left(\frac{\partial t}{\partial y}\right)_{y=0} = -k(t_w - t_e)\frac{1}{2}\sqrt{\left(\frac{u_e}{\nu x}\right)}\left\{\theta_0' + \epsilon_1(x)\,H_1' \pm \frac{\epsilon_1(x)\,I_1'}{\sqrt{[Re(x)]}}\right\}_{\eta=0} \quad (30)$$

In equations (27), (28), (29), and (30) the + sign is used when ϵ_1 and ϵ_2 are of similar sign and the − sign is used when ϵ_1 and ϵ_2 are of different sign [see equations (19) and (20) and Appendix].

RESULTS

Equations (21), (22), (23), (24), (25) and (26), with boundary conditions (18), were solved for wedge angles ranging from $1{\cdot}0 \geqq \beta \geqq -0{\cdot}190$. The Prandtl number, Pr, was taken to equal 0·73, a value typical for air. The solutions were found numerically by using the Runge–Kutta method on a Burroughs 220 computer. The error in the calculations was estimated by changing the interval of integration. The calculations were thus found to be accurate to the sixth significant figure and are shown tabulated to the fourth decimal place.

With reference to equations (27), (28), (29) and (30), it was found that for some wedge angles in both Cases A and B the $G_1/\sqrt{[Re(x)]}$ and $I_1/\sqrt{[Re(x)]}$ terms were insignificant in magnitude relative to the corresponding F_1 and H_1 terms in view of the large Reynolds number for boundary-layer flow. This was found true in Case A for wedge angles of $\beta \geqslant 0{\cdot}5$ and for all the wedge angles considered in Case B. However, in Case A, for wedge angles of $\beta < 0{\cdot}5$, the $G_1/\sqrt{[Re(x)]}$ and $I_1/\sqrt{[Re(x)]}$ terms, with the exception of the horizontal flat plate case, were found to be a factor of $1/\sqrt{[Re(x)]}$ times smaller than the F_1 and H_1 terms but tended to offer a small contribution in equations (27), (28), (29), and (30) for Reynolds number in the lower portion of the permissible boundary layer range. In the case of the horizontal flat plate, the F_1 and H_1 terms become zero and the $G_1/\sqrt{[Re(x)]}$ and $I_1/\sqrt{[Re(x)]}$ terms represent the only influence of

buoyancy. Thus for $\beta \geqq 0{\cdot}5$ in Case A and for all β in Case B, equations (22) and (25) were alone calculated. For the remaining wedge angles in Case A equations (23) and (26) were in addition calculated.

Figure 2 shows the mixed flow velocity and thermal distribution for a $\beta = 0{\cdot}5$ wedge of Case A where $\epsilon_1 = -0{\cdot}3$. The $\epsilon_1 = 0$ curve represents the purely forced flow distribution [i.e. $Gr(x) = 0$].

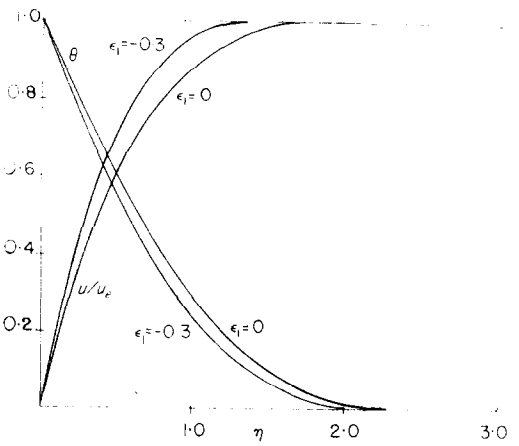

FIG. 2. Velocity and temperature profiles for a $\beta = 0{\cdot}5$ wedge for Case A.

If the purely forced flow local shear stress and heat-transfer rate are denoted by $\tau_0(x)$ and $\dot{q}_0''(x)$, the ratios of the local shear stress and local heat transfer for the flow with buoyancy to the purely forced convection flow can be obtained.

$$\frac{\tau}{\tau_0}(x) = \left\{1 + \epsilon_1(x)\left[\left(\frac{F_1''}{f_0''}\right)_{\eta=0} \pm \frac{1}{\sqrt{[Re(x)]}}\left(\frac{G_1''}{f_0''}\right)_{\eta=0}\right]\right\} \quad (31)$$

$$\frac{\dot{q}''}{\dot{q}_0''}(x) = \left\{1 + \epsilon_1(x)\left[\left(\frac{H_1'}{\theta_0'}\right)_{\eta=0} \pm \frac{1}{\sqrt{[Re(x)]}}\left(\frac{I_1'}{\theta_0'}\right)_{\eta=0}\right]\right\} \quad (32)$$

where the + sign is used when ϵ_1 and ϵ_2 are of the same sign and the − sign is used when ϵ_1 and ϵ_2 are of opposite sign (see Appendix).

Equations (31) and (32) can be integrated over a length, L, of the wedge surface to obtain the drag and heat-transfer rate for the portion of the wedge surface $0 \leqslant x \leqslant L$. These quantities are written in terms of the total drag coefficient and Nusselt number to yield:

$$\frac{C_D}{C_{D_0}} = \left[1 + \epsilon_1(L)(3m + 1)\left(\frac{F_1''}{f_0''(3 + m)} \pm \frac{G_1''}{f_0''(2 + 2m)\sqrt{[Re(L)]}}\right)_{\eta=0}\right] \quad (33)$$

$$\frac{Nu}{Nu_0} = \left[1 + \epsilon_1(L)(3m + 1)\left(\frac{H_1'}{\theta_0'(3 - 3m)} \pm \frac{I_1'}{\theta_0'(2 - 4m)\sqrt{[Re(L)]}}\right)_{\eta=0}\right] \quad (34)$$

where the subscript "0" refers to the purely forced flow quantity and

$$C_D = \frac{2\int_0^L \tau(x)\,dx}{L\rho_e u_e^2(L)} \text{—drag coefficient}$$

$$Nu = \frac{\int_0^L \dot{q}''(x)\,dx}{(t_w - t_e)k} \text{—Nusselt number}$$

Again the + sign is used when ϵ_1 and ϵ_2 are of the same sign and the − sign is used when ϵ_1 and ϵ_2 are of opposite sign. Values of

$$\left(\frac{F_1''}{f_0''}\right)_{\eta=0}, \quad \left(\frac{G_0''}{f_0''}\right)_{\eta=0}, \quad \left(\frac{H_1'}{\theta_0'}\right)_{\eta=0} \text{ and } \left(\frac{I_1'}{\theta_0'}\right)_{\eta=0}$$

are shown tabulated for the appropriate range of wedge angles.

The effect of buoyancy on separation may be determined from the computed results. The condition for boundary-layer separation from the wedge surface is met when the flow tends to reverse at the interface. This condition first occurs when

$$\left(\frac{\partial u}{\partial y}\right)_{y=0} = 0 \quad (35)$$

For pure forced convection (in the absence of buoyancy effects) Hartree found that this condition was met for a wedge of included angle of $-35{\cdot}64°$ or $\beta = -0{\cdot}1988$.

Table 1. Tabulated results for Case A

β	$(f_0'')_{\eta=0}$	$(\theta_0')_{\eta=0}$	$(F_1''/f_0'')_{\eta=0}$	$(G_1''/f_0'')_{\eta=0}$	$(H_1'/\theta_0')_{\eta=0}$	$(I_0'/\theta_0')_{\eta=0}$	$\epsilon_{1_s}(x)$
1·0	4·93035	−1·00836	−0·4952		0·0000		2·0194
0·8	4·09064	−0·90448	−0·6361		−0·0678		1·5721
0·7	3·71805	−0·86006	−0·6928		−0·1359		1·4434
0·5	3·02979	−0·78080	−0·7547		−0·1737		1·3203
0·1	1·70353	−0·63561	−0·4391	−3·0849	−0·1048	−0·7487	2·2774
0·0	1·32823	−0·59418	−0·0000	−5·0737	−0·0000	−1·1959	$(0{\cdot}1971)\sqrt{[Re(x)]}$
−0·1	0·88128	−0·54179	−1·0520	−10·5898	−0·2196	−2·2566	0·9506
−0·15	0·59024	−0·50390	−2·8887	−21·1421	−0·5300	−3·9062	0·3462
−0·175	0·39642	−0·47570	−6·2807	−42·1402	−0·9772	−6·4970	0·1592
−0·180	0·34853	−0·46821	−7·9394	−52·8078	−1·1624	−7·6153	0·1260
−0·185	0·29479	−0·45940	−10·7212	−70·9885	−1·4407	−9·3283	0·0933
−0·190	0·23168	−0·44880	−16·4464	−109·195	−1·9304	−12·4069	0·0608

In the case of mixed flow, values of ϵ_1 for which equation (35) is satisfied is found from equation (27) as

$$\epsilon_{1_s}(x) = \left(\frac{f_0''}{F_1'' \pm \dfrac{G_1''}{\sqrt{[Re(x)]}}} \right)_{\eta=0} \tag{36}$$

where $\epsilon_{1_s}(x)$ is the value of $\epsilon_1(x)$ that causes separation of the flow. Values of $\epsilon_{1_s}(x)$ are tabulated for Cases A and B. For purposes of illustration, the

$$\left(\frac{G_1''}{\sqrt{[Re(x)]}} \right)_{\eta=0}$$

term is neglected in equation (36), except for $\beta = 0$ in Case A.

In Fig. 3 are shown plotted velocity distributions for the wedge angle of $\beta = -0{\cdot}180$ for Case A. The separation tendency can be seen as ϵ_1 is increased from zero to the value ϵ_{1_s} where the initial slope is zero. For $\epsilon_{1_s}(x) > \epsilon_1(x) = 0{\cdot}1260$, reversed flow is shown.

For all the other wedge profiles the local shear stress and heat transfer are seen to be increased by the effects of buoyancy when $\epsilon_1 < 0$ and decreased for $\epsilon > 0$ (see Appendix).

Table 2. Tabulated results for Case B

β	$(F_1''/f_0'')_{\eta=0}$	$(H_1'/\theta_0')_{\eta=0}$	$\epsilon_{1_s}(x)$
1·0	0·0000	0·0000	∞
0·8	−0·2067	−0·0336	4·8379
0·7	−0·3530	−0·0692	2·8329
0·5	−0·7547	−0·1737	1·3203
0·1	−2·4973	−0·5961	0·4004
0·0	−3·6526	−0·8392	0·2738
−0·1	−6·6426	−1·3867	0·1505
−0·19	−53·4595	−6·2748	0·0187

The tabulated values show that only for values of $\epsilon_1(x) > 0$ do the effects of buoyancy contribute to the separation phenomena. These values thus set an upper limit to the $Gr(x)/Re^2(x)$ parameter such that flow separation does not

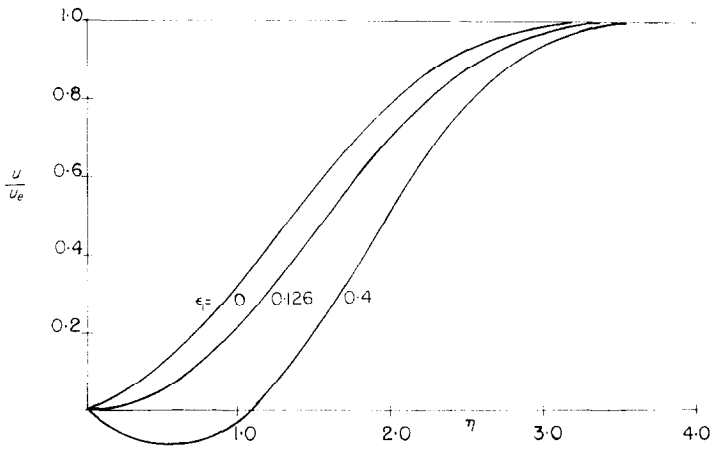

FIG. 3. Separation phenomena for a $\beta = -0{\cdot}180$ wedge for Case A.

occur. Values of $\epsilon_1(x)$ can apparently have any negative value and not influence separation.

CONCLUSIONS

From the results, certain generalizations are possible concerning the effects buoyancy has in the mixed flow regime.

One of the more interesting matters to consider is the manner in which thermal changes in the x and y body forces of the fluid elements influence the flow. In equation (10), it is seen that the $\partial\theta/\partial y$ term stems from changes in the x body force while the $\partial\theta/\partial x$ term stems from changes in the y body force. By non-dimensionalizing these terms and applying the conventional boundary-layer arguments, it is found that the ratio of these terms become

$$\frac{g_x B(t_w - t_e)\,\partial\theta/\partial y}{g_x B(t_w - t_e)\,\partial\theta/\partial x} = O\left[\frac{g_x\sqrt{[Re(x)]}}{g_y}\right] \quad (37)$$

where O denotes "order of magnitude".

For the wide range of wedge angles where $g_x \simeq O(g_y)$ (remembering that $Re(x) \gg 1$ for the boundary layer equations to be valid), it is seen that the $\partial\theta/\partial y$ term, or the contribution due to changes in the x component of the body force, is far greater than the $\partial\theta/\partial x$ term which comes from changes in the y component.

Since the $\partial\theta/\partial x$ term in equation (10) comes from differentiating equation (3) with respect to x, it is also seen the $\partial(\partial p/\partial y)/\partial x$ will likewise be very small. This means, as is the case in the purely forced flow, that the pressure gradient in the x-direction is essentially that of the invisid free stream value. It is noted that the free stream pressure gradient is taken as the same for both the mixed and forced flow.

From equation (8), however, it is seen that the body force in the x-direction is different than that of the purely forced flow body force. When $t_w > t_e$, this body force is seen to be less and for $t_w < t_e$ it is seen to be greater than the purely forced flow value. Since the x-direction pressure gradient in the boundary layer is essentially the same in both flows, the fluid elements in the combined flow experience a net retarding or acceleration force not experienced in the pure flow. This net force is thus due to the weakening or strengthening of the x-direction body force with respect to the pure flow values.

For flow circumstances where g_x is in the negative x-direction and the wedge is heated, (i.e. $t_w > t_e$), then the x-direction body force is lessened by decreasing density and the fluid appears to have a net force in the positive x-direction which tends to speed up the flow. The opposite effects would then be expected if g_x were positive or if $t_w < t_e$.

It is important to note that a net convective force does not exist in the y-direction. The reason for this is due to the boundary-layer approximation made in equation (3). Thus the only way changes in the y-body force can influence the flow is by the small changes in the

x-direction pressure gradient relative to the external flow gradient. For the larger wedge angles, this effect is negligible compared to the effect induced by the changes in the x body force. However, in Case A, for the smaller wedge angles, the x body force becomes relatively smaller and the changes in the pressure field, due to the variation in the y body force, tend to offer a slight contribution or correction term (usually in the third significant figure) when the results are applied. For the case of the horizontal flat plate, the x body force becomes zero and the small effect of the variation of the pressure field is the only way buoyancy can influence the flow. However, the effect is still $1/\sqrt{[Re(x)]}$ times smaller than for a comparable effect in the other angles.

From the Tables, certain conclusions can be drawn concerning the influence buoyancy has on boundary-layer separation. As was previously indicated, for the case of the purely forced flow Hartree found that only wedges where $\beta \leqslant -0{\cdot}1988$ caused the boundary layer to separate from the wedge surface. The presence of buoyancy, however, is seen to cause separation for any wedge angle provided that

$$\epsilon_1(x) \geqslant \epsilon_{1_s}(x) > 0,$$

within the limits of this perturbation analysis. It can be concluded that positive $\epsilon_1(x)$ tend to bring the flow closer to separation whereas negative values of $\epsilon_1(x)$ tend to stabilize the flow. The negative wedge angle flows are much closer to a separation condition than the positive wedge flows and much smaller values of $\epsilon_{1_s}(x)$ are required to cause separation.

Several of the specific cases included in this analysis have been treated by other investigators. The vertical plate problem, considered by [2], [3], and [4] corresponds to Case B, Fig. 1, where the included wedge angle, β, is zero. The present results are in agreement with those previously reported. Likewise, the horizontal flat plate case considered by [5] and [6] agree with the results obtained for $\beta = 0$ in Case A.

The wedge having an included angle of 120° was not calculated in this work. Therefore, the similarity analysis by Sparrow, Eichhorn and Gregg [8] for this wedge angle was compared to our results for $\beta = 0{\cdot}7$ or $\pi\beta = 126°$. With consideration given to the slight change in wedge angle, the results were found to be in excellent agreement. Since the Sparrow, Eichhorn and Gregg analysis is valid for all values of $\epsilon_1(x)$, some idea of the permissible magnitude of this parameter was gained by comparison of results. As was expected, for values of $\epsilon_1(x) < 1$, agreement between the perturbed and exact solution was found to the third significant figure. For values of $\epsilon_1(x) > 1{\cdot}0$, however, the higher order terms in equations (16) and (17) become increasingly important. Therefore, it may be expected that the results presented herein are reliable at large values of $\epsilon_1(x)$ only as indications of the effect of buoyancy on forced convection.

REFERENCES

1. A. A. TANAEV, Effect of free convection on the coefficient of resistance of a plate with a laminar flow regime in the boundary layer, *Sov. Phys. Tech. Phys.* **1**, 2477 (1956).
2. A. ACRIVOS, Combined laminar free and forced convection heat transfer in external flow, *J. Amer. Inst. Chem. Engrs* **4**, 285 (1958).
3. E. M. SPARROW and J. L. GREGG, Buoyancy effects in forced convection flow and heat transfer, *Trans. Amer. Soc. Mech. Engrs* **E81**, 133 (1959).
4. A. A. SZEWCZYK, Combined forced and free-convection laminar flow. ASME Paper 63-*WA*-130, 1963.
5. Y. MORI, Buoyancy effects in forced laminar convection flow over a horizontal flat plate, *Trans. Amer. Soc. Mech. Engrs* **C82**, 479 (1961).
6. E. M. SPARROW and W. J. MINKOWYCZ, Buoyancy effects on horizontal boundary-layer flow and heat transfer, *Int. J. Heat Mass Transfer* **5**, 505 (1962).
7. W. H. GILL and E. DEL CASEL, A theoretical investigation of natural convection effects in forced horizontal flows, *J. Amer. Inst. Chem. Engrs* **8**, 513 (1962).
8. E. M. SPARROW, R. EICHHORN and J. L. GREGG, Combined force and free convection in a boundary layer flow, *Phys. Fluids* **2**, 319 (1959).
9. J. BRINDLEY, An approximate technique for natural convection in a boundary layer, *Int. J. Heat Mass Transfer* **6**, 1035 (1963).
10. V. M. FALKNER and S. W. SKAN, Some approximate solutions of the boundary layer equations, *Phil. Mag.* **12**, 865 (1931).
11. E. ECKERT, Die Berechnung des Wärmeübergangs in der Laminaren Grenzschicht, *VDI—Forsch.* **416** (1942).

APPENDIX

It is necessary to evaluate the constants γ and λ defined by

$$g_x = \pm \gamma |g| \tag{38}$$

$$g_y = \pm \lambda |g| \tag{39}$$

For Case A, Fig. 1, the components of gravity are seen to be

$$g_x = \pm \gamma |g| = \pm |g| \sin\left(\frac{\pi\beta}{2}\right) \tag{40}$$

$$g_y = \pm \lambda |g| = \pm |g| \cos\left(\frac{\pi\beta}{2}\right) \tag{41}$$

Thus for Case A:

$$\gamma = \sin\left(\frac{\pi\beta}{2}\right) \tag{42}$$

$$\lambda = \cos\left(\frac{\pi\beta}{2}\right) \tag{43}$$

For Case B, Fig. 1, the following is seen to be true

$$g_x = \pm \gamma |g| = \pm |g| \cos\left(\frac{\pi\beta}{2}\right) \tag{44}$$

$$g_y = \pm \lambda |g| = \pm |g| \sin\left(\frac{\pi\beta}{2}\right) \tag{45}$$

Thus for Case B:

$$\gamma = \cos\left(\frac{\pi\beta}{2}\right) \tag{46}$$

$$\lambda = \sin\left(\frac{\pi\beta}{2}\right) \tag{47}$$

As a matter of convenience, λ and γ are always taken as positive. In equations (38) and (39) the $\pm$ sign is determined from the case being considered. When the direction of g_x is opposite to that of the increasing x-axis, the $-$ sign is used in equation (38). When g_x is in the direction of increasing x, the $+$ sign is used. In a similar manner, the $+$ sign of g_y, equation (39), is determined by the orientation of g_y relative to the y-axis.

The same holds true for equations (19) and (20). Since

$$Gr(x) = \pm \frac{|g| B(t_w - t_e)\, x^3}{\nu^2}$$

it is seen that the $+$ sign is used in equation (19) when g_x is positive and the $-$ sign used when g_x is negative. In equation (20) the $+$ sign is used when g_y is positive and the $-$ sign when g_y is negative.

These remarks on the sign convention lead to the following generalizations. For $t_w > t_e$, the sign of ϵ_1 is the same as the sign of g_x. Similarly, the sign of ϵ_2 is always the sign of g_y. The opposite holds true for both ϵ_1 and ϵ_2 when $t_e > t_w$.

Résumé—Cet article considère simultanément les phénomènes des effets de l'écoulement forcé et natural sur un dièdre isotherme. L'analyse est restreinte aux situations dans lesquelles les effets de convection naturelle peuvent être considérés comme une perturbation de la situation avec un écoulement purement forcé. En utilisant cette technique, un certain nombre d'angles de dièdres est considéré pour un écoulement du type couche limite laminaire. Un nombre de Prandtl de 0,73 a été employé et les résultats numériques sont présentés pour calculer la tension de cisaillement pariétal et les flux de transport de chaleur. Le décollement de la couche limite est aussi considéré.

Zusammenfassung—Diese Abhandlung betrachtet gleichzeitig die Vorgänge bei erzwungener und freier Konvektionsströmung über einen isothermen Keil. Die Untersuchung beschränkt sich auf Zustände, bei denen die freie Konvektion als eine Störung der reinen erzwungenen Konvektionsströmung betrachtet wird. Mit dieser Technik werden eine Anzahl von Keilen mit verschiedenen Winkeln bei Strömungen mit laminarer Grenzschicht untersucht. Die Prandtl-Zahl betrug 0,73. Für die Berechnung der Schubspannung und des Wärmeüberganges werden numerische Ergebnisse aufgeführt. Die Grenzschichtablösung wurde ebenfalls berücksichtigt.

Аннотация—В статье исследуются явления совместной вынужденной и свободной конвекции при обтекании изотермического клина. Теоретический анализ ограничен случаем, когда эффекты свободной конвекции рассматриваются как возмущения чисто

вынужденного течения. С помощью данной методики исследован ряд углов клина при течении типа ламинарного пограничного слоя. Использовалось число Прандтля 0,73. Приводятся многочисленные данные для расчета поверхностного трения и теплообмена. Рассмотрен также отрыв пограничного слоя.